Supplemental Figures:

Fig. S1. Anti-HIV activity of HP23 compared to MT-SC22EK. (A) Inhibition of HIV-1_{HXB2} Env-mediated cell-cell fusion. **(B)** Inhibition of HIV-1_{NL4-3} pseudovirus entry. **(C)** Inhibition of wild-type HIV-1_{NL4-3} infection. Percentage inhibition of the peptides and IC_{50} values were calculated as described. Data were derived from the results of 3 independent experiments, and the results are expressed as the means ± S.D.

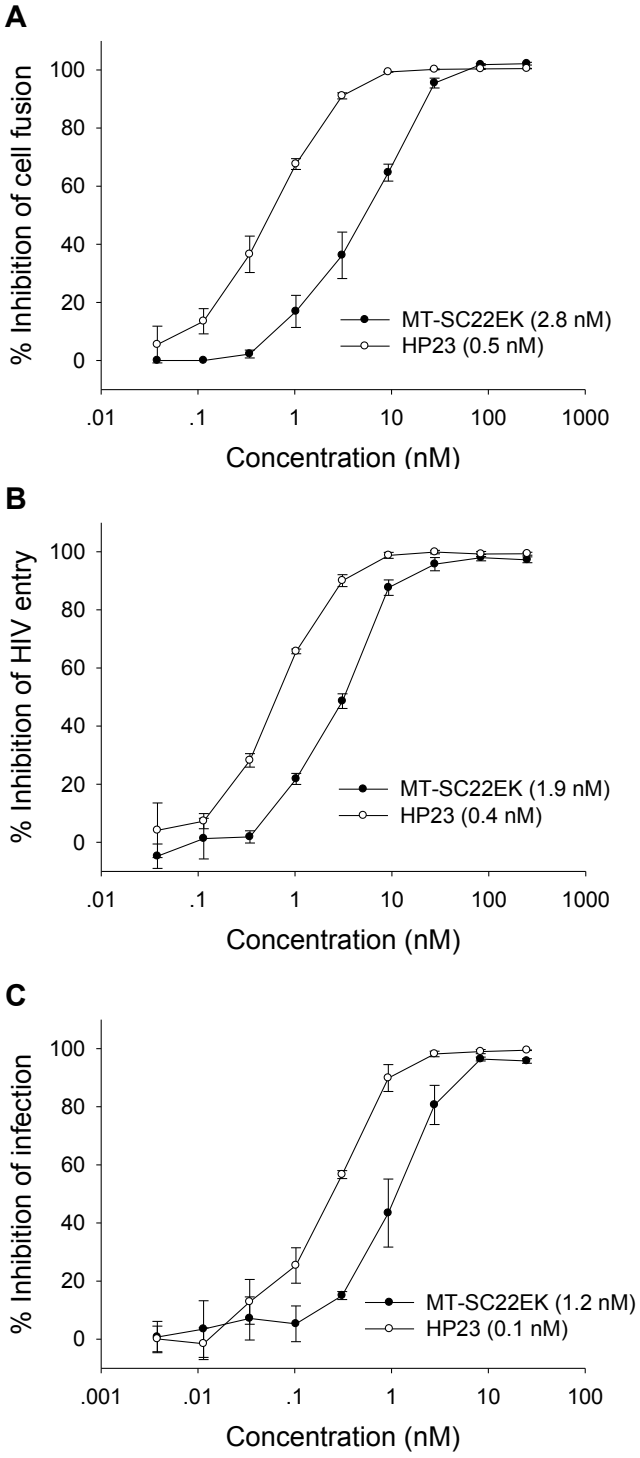

Fig. S2. Binding stability of HP23 and MT-SC22EK with N36 mutants determined using CD spectroscopy. (A) I37T; **(B)** V38A; **(C)** Q40H; **(D)** N43K; **(E)** I37T/N43K; **(F)** V38A/N42T. Final concentration of each peptide in PBS is 10 μM.

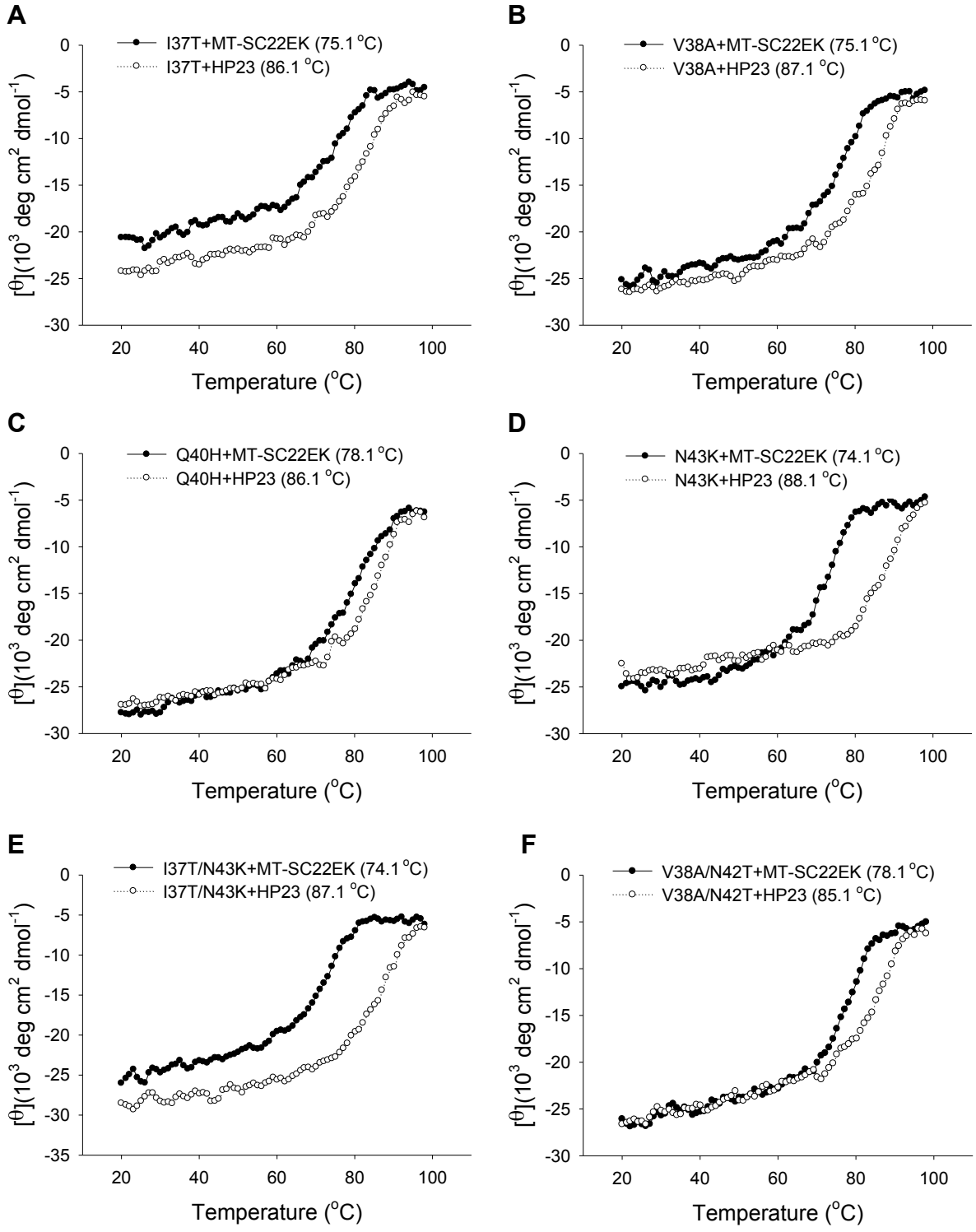

Fig. S3. ***In vitro*** **selection of HIV-1 resistant to fusion inhibitors.** The molecular clone of HIV-1_{NL4-3} was passaged in the presence of 1.5- to 2-fold escalating concentrations of peptides. HP23 and MT-SC22EK failed to select HIV-1 resistant to inhibitors compared with SC22EK.

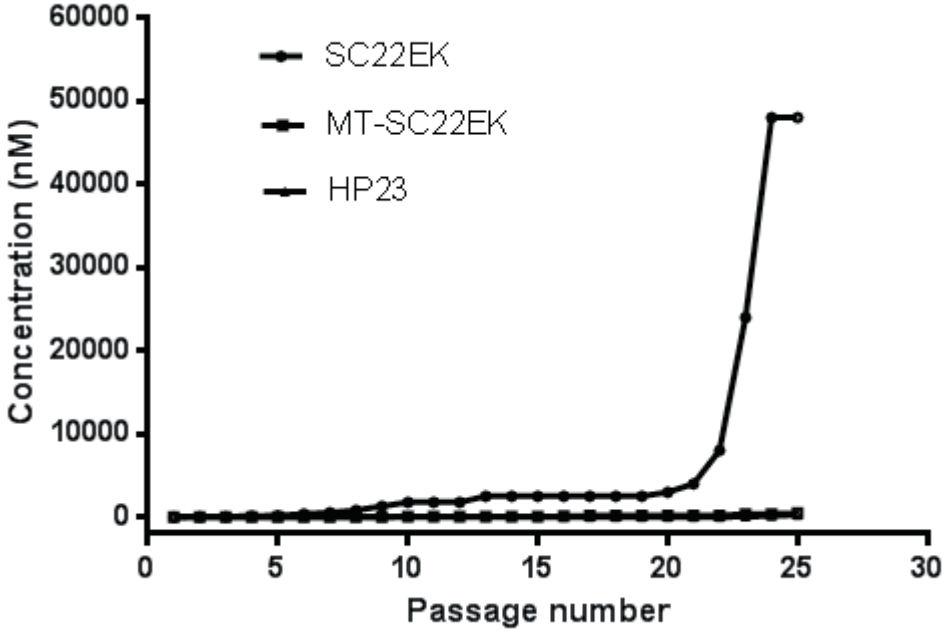

Supplemental Table S1:

Table S1. Inhibitory activity of HP23 against primary HIV-1 subtypes[a]

		IC_{50} (nM)		
Pseudovirus	Subtype	C34	MT-SC22EK	HP23
92RW020	A	3.1 ± 0.8	3.4 ± 0.4	1.1 ± 0.2
92UG037.8	A	3.0 ± 0.5	3.4 ± 0.3	0.9 ± 0.1
SF162	B	9.5 ± 1.4	9.4 ± 2.4	2.4 ± 0.7
AC10.0.29	B	1.5 ± 0.4	1.6 ± 0.2	0.7 ± 0.1
TRO.11	B	4.4 ± 1.2	12.9 ± 1.3	2.2 ± 0.5
REJO4541	B	0.7 ± 0.1	3.0 ± 1.0	0.6 ± 0.2
SC422661.8	B	0.5 ± 0.0	4.4 ± 0.5	0.6 ± 0.1
B01	B'	1.2 ± 0.1	18.0 ± 1.9	1.5 ± 0.3
ZM214M.PL15	C	3.4 ± 0.6	5.0 ± 1.5	1.2 ± 0.5
ZM109F.PB4	C	1.8 ± 0.3	1.2 ± 0.2	0.6 ± 0.1
CAP45.2.00.G3	C	13.2 ± 1.1	10.6 ± 3.6	2.0 ± 0.3
AE01	A/E	2.7 ± 0.1	2.6 ± 0.5	0.7 ± 0.2
AE03	A/E	3.0 ± 0.7	4.4 ± 1.2	1.1 ± 0.3
GX11.13	A/E	8.2 ± 1.1	11.9 ± 1.8	2.2 ± 0.8
CH64.20	B/C	1.1 ± 0.1	1.0 ± 0.1	0.4 ± 0.1
CH070.1	B/C	5.1 ± 0.4	5.0 ± 1.7	2.1 ± 0.3
CH120.6	B/C	3.5 ± 0.8	9.4 ± 1.9	2.5 ± 0.6

[a]The IC_{50} data were derived from the results of three independent experiments and expressed as means ± SD.